Dual-Population Social Group Optimization Algorithm Based on Human Social Group Behavior Law

Chao Wang, Xianqi Zhang, Yi Niu, Shan Gao, Jing Jiang, Zezhan Zhang, Peifeng Yu, and Hairong Dong, *Senior Member, IEEE*

***Abstract*— Inspired by the behavior law of human social groups, a new swarm intelligence algorithm named the dual-population social group optimization (DPSGO) algorithm is proposed in this article. Based on the primitive social group optimization (SGO) algorithm, dual-population grouping technology, reverse learning technology, immigration migration technology, and Gaussian mutation are introduced to further simulate the behavior law of actual human social groups. Experimental results and performance comparison show that the DPSGO algorithm has a better searchability and convergence rate. In addition, aiming at the socially hot issue of aviation safety, the simulation and experimental results show that the temperature measurement error can be reduced to less than 7.5 °C by using the DPSGO algorithm combined with reflected radiation correction to process the aeroengine multispectral radiation temperature measurement data. This article is of great significance to the design and optimization of swarm intelligence algorithms by using the behavior law of human social groups and provides valuable guidance for enhancing the safety monitoring of aeroengines.**

***Index Terms*— Dual-population social group optimization (DPSGO) algorithm, human social group behavior, multispectral radiation temperature measurement, social group optimization (SGO) algorithm.**

Manuscript received August 13, 2021; revised December 4, 2021; accepted December 30, 2021. This work was supported in part by the National Key Research and Development Program of China under Grant 2017YFC0602102; in part by the National Natural Science Foundation of China under Grant U20A20213, Grant 61727818, and Grant 61805056; in part by the Department of Science and Technology of Sichuan Province under Grant 2021JDTD0030; in part by Chengdu Science and Technology Project under Grant 2020-GH02-0065-HZ; in part by Aero Engine Corporation of China (AECC) Sichuan Gas Turbine Research Establishment under Grant WDZC-2020-3-2; and in part by Fundamental Research Funds for the Central Universities under Grant 3072021CFT0802. *(Chao Wang, Xianqi Zhang, and Yi Niu are co-first authors.) (Corresponding authors: Chao Wang; Shan Gao; Jing Jiang.)*

Chao Wang, Yi Niu, Jing Jiang, Zezhan Zhang, and Peifeng Yu are with the Clean Energy Materials and Engineering Center, School of Electronic Science and Engineering, State Key Laboratory of Electronic Thin Film and Integrated Devices, University of Electronic Science and Technology of China, Chengdu 611731, China (e-mail: cwang@uestc.edu.cn; niuyi@uestc.edu.cn; jiangj@uestc.edu.cn; 18637401828@163.com; yu605898922@163.com).

Xianqi Zhang and Shan Gao are with the Key Laboratory of Advanced Marine Communication and Information Technology, Ministry of Industry and Information Technology, School of Information and Communication Engineering, Harbin Engineering University, Harbin 150001, China (e-mail: zhangxianqi@hrbeu.edu.cn; gaoshan08@hrbeu.edu.cn).

Hairong Dong is with the State Key Laboratory of Rail Traffic Control and Safety, Beijing Jiaotong University, Beijing 100044, China (e-mail: hrdong_pcm@outlook.com).

Digital Object Identifier 10.1109/TCSS.2022.3141114

I. Introduction

THE intelligence algorithm is a new optimization method of abstracting mathematical models from laws and cooperative behaviors existing in nature or biological groups in order to obtain powerful problem-solving abilities. In nature, many organisms complete complex tasks together through group collaboration and the simple behaviors of individuals in a group display intelligence due to the interaction between individuals. The existing swarm intelligence algorithms are mostly abstracted and extended by simulating group behaviors of animals, such as social insects, animals, and birds [1], [2]. Typical optimization algorithms include ants [3], fireflies [4], and bats [5]. Swarm intelligence algorithms have a wide range of practical applications. The reliability-based design optimization (RBDO) is an effective method for structural optimization due to its capability of consideration of uncertainties in design variables [6]. Meng *et al.* [7] made a comprehensive comparison of recent metaheuristics algorithms for the application of RBDO through five mechanical design problems: automobile side impact problem, bolted rim, spur speed reducer, welded beam, and stiffened shell. Dhiman *et al.* [8] proposed an evolutionary multiobjective seagull optimization algorithm (EMoSOA) and used the proposed EMoSOA algorithm to verify four engineering design problems, including welded beam design and pressure vessel design. Aiming at the design problem of unmanned aerial vehicles, Champasak *et al.* [9] proposed a new self-adaptive metaheuristic based on decomposition. Dhiman *et al.* [10] proposed a novel bioinspired optimization algorithm called rat swarm optimizer (RSO) and applied it to six real-life constrained engineering design problems. Abd Elaziz *et al.* [11] used swarm intelligence algorithms for medical image processing. However, as humans have the highest level of intelligence among biological groups, the evolution process of human social intelligence has good reference significance. Human beings are social creatures, and their social systems are composed of many people with dynamic and adaptive behaviors. People interact through the establishment of relationships [12]. According to the research and verification of scholars, the complex behavior of social group systems can be modeled and simulated by computer. Inspired by the evolution process of human intelligence

and the social learning theory [13], Liu *et al.* [14] proposed a new swarm intelligence algorithm paradigm named the social learning optimization (SLO) algorithm. Based on human intelligence with the social cognitive theory (SCT), Xie *et al.* [15] proposed social cognitive optimization (SCO) for solving nonlinear programming problems (NLP). Sun *et al.* [16] proposed a novel hybrid SCO algorithm based on quantum behavior (QSCO) to improve the global convergence speed of the classical SCO algorithm. Gong *et al.* [17] developed a social learning algorithm (SLA) by imitating the social learning process of humans in society. Based on social ties, Lin *et al.* [18] constructed a social effect-based incentive mechanism and a social graph model with social ties. Cao *et al.* [19] made full use of the location and semantic information of social networks to propose a review-based local expert discovery mechanism. At present, research into a swarm intelligence algorithm model based on the evolution process of human swarm intelligence is still in its infancy.

The social group optimization (SGO) algorithm is a new type of optimization algorithm based on the human behavior of learning and solving complex problems. The process of SGO is divided into two parts. The first part consists of the "improving phase"; the second part consists of the "acquiring phase." In the "improving phase," individuals in the population take the current optimal solution of the group as the learning guide. In the "acquiring phase," individuals in the population learn under the guidance of a random individual in the population and the optimal solution of the current population. The SGO algorithm has a fast convergence speed and strong effectiveness [20]. It has effective research applications in many fields, such as medical image processing [21]–[23], resource allocation task scheduling [24], and information processing communication technology [25]–[27]. With advancing research on the laws of human social group behavior, it has been found that the SGO algorithm can be optimized and achieve better results when combined with actual human group social behavior. Studies have demonstrated that people in geographically similar areas in human social groups often showed behavioral similarities. Compared to individuals who were further away, people were found to be more inclined to contact individuals with closer geographical locations [28], [29]. With the widespread dissemination of mobile Internet technologies that include mobile phones, smart terminals, and wearable devices, as well as the popularization of Facebook, Twitter, Microblogging, and other online social networks, the restrictions of traditional social networks on individual time and space have been removed [30]–[32]. Therefore, we introduce the dual-population grouping operation and optimize the update mode of the algorithm to simulate this social group phenomenon. At the same time, considering that individuals in actual human social groups still have deliberative and autonomous learning behaviors, reverse learning technology is introduced. In addition, the migration operation between populations is used to simulate the flow of people in different social groups, and the Gaussian mutation operation is employed to simulate the strong self-learning ability of excellent individuals. We present the dual-population social group optimization (DPSGO) algorithm in this work, which is based on the above factors.

Due to economic and social progresses, and particularly in the context of globalization, countries are becoming integrated, including in the economic and cultural spheres [33]. In addition, while aviation technology has been widely adopted, aviation safety continues to be a culturally significant concern. Turbine blades are one of the key components of aeroengines. Accurately measuring the temperature of turbine blades is of great importance for ensuring the safe operation of aeroengines. Turbine blade radiation temperature measurement experiences the problems of reflection radiation interference between blades and insufficient accuracy and stability of the multispectral temperature measurement data processing algorithm. In response to these specific problems, we conduct simulation analysis and experimental verification on the effectiveness of the DPSGO algorithm for processing multispectral radiation temperature measurement data of aeroengines. The experimental results and performance comparison show that the DPSGO algorithm is both effective and efficient. The use of temperature to monitor the operational safety of aeroengines can also reduce aviation safety concerns.

II. Basic Principle of SGO Algorithm

Many behavioral traits, such as honesty, courage, tolerance, or respectfulness, lie dormant in human beings, which must be harnessed and channelized in the appropriate direction to solve complex tasks. A phenomenon of mutual influence on the emotions or abilities of others in the process of interpersonal communication also exists in social groups [34]. It has been observed that human beings are great imitators or followers when solving tasks. Group solving capability is now recognized as more effective than individual capability due to the exploiting and exploring of different traits of each individual in a group to solve a given problem. A new optimization technique has been proposed based on this concept, named SGO [35]. In the SGO algorithm, everyone can acquire knowledge and has a certain degree of problem-solving ability. The optimal individual can determine the best solutions and will attempt to spread knowledge among all individuals, which will improve the knowledge level of all team members.

The SGO algorithm is an optimization algorithm based on social group learning. Similar to particle swarm algorithms, it mimics social behavior, such as adaptation based on interaction with others to reduce differences and the ability to use historical knowledge in present behaviors and decisions [36]. After the social group is initialized, the individual optimization process is divided into the "improving phase" and the "acquiring phase." In the "improving phase," the knowledge level of each person in the group is improved under the influence of the outstanding people in the group. In the "acquisition phase," each person enhances their knowledge by communicating with other people in the group and the best people in the group. The algorithm is described as follows.

Step 1: The population initialization operation is given as follows:

$$X_{i,j} = x_{\min} + r \times (1, D) \times (x_{\min} - x_{\max}) \tag{1}$$

where $i = 1, 2, 3, \ldots, N$, $j = 1, 2, 3, \ldots, D$, N is the size of the population, D is the dimensionality of individual variables, and r is a random number of between 0 and 1. $x_{\max}$ and $x_{\min}$ are the upper and lower limits of variables, respectively; $X_{i,j}$ is the feature number of the jth dimension of individual i.

Step 2: The improving phase is given as follows:

$$X_{\text{new}_{i,j}} = c \times X_{\text{old}_{i,j}} + r \times (\text{gbest}_j - X_{\text{old}_{i,j}}) \tag{2}$$

where c is known as the self-introspection parameter and its value can be set from 0 to 1. r is a random number of 0–1, gbest_j is the jth dimension feature number of the optimal individual of the current generation, and $X_{\text{old}_{i,j}}$ and $X_{\text{new}_{i,j}}$ are the jth dimension feature numbers before and after the update of individual i, respectively.

Step 3: The acquiring phase is given as follows:

$$\begin{aligned}&\text{if } f(x_i) \text{ is better than } f(x_k)\\ &\quad X_{\text{new}_{i,j}} = X_{\text{old}_{i,j}} + r_1 \times (X_{i,j} - X_{k,j}) + r_2 \times (\text{gbest}_j - X_{i,j})\\ &\text{else}\\ &\quad X_{\text{new}_{i,j}} = X_{\text{old}_{i,j}} + r_1 \times (X_{k,j} - X_{i,j}) + r_2 \times (\text{gbest}_j - X_{i,j})\end{aligned} \tag{3}$$

where both r_1 and r_2 are random numbers between 0 and 1, X_k is an individual randomly selected from the population as the learning object, gbest_j is the jth dimension feature number of the optimal individual of the current generation, and $f(x)$ is the individual fitness evaluation function, which is used to evaluate the level of knowledge and ability.

Step 4: Termination criterion.

Stop the simulation if the maximum generation number is achieved; otherwise, repeat steps 2–3.

III. Basic Principle of DPSGO Algorithm

While the original SGO algorithm shows the effectiveness and rapid convergence in some applications, it still has some shortcomings. In the two stages of the original SGO algorithm, individuals are updated under the guidance of the best individuals of the contemporary population. Practice shows that guiding evolution with the optimal individual can accelerate the convergence speed of the algorithm, but it is not conducive to maintaining the diversity of the population. Employing a single algorithm learning method can also easily lead to premature convergence. Therefore, in response to the above problems and combined with the actual human social group behavior law, a DPSGO algorithm is proposed in this work. The improvement points and analysis of the DPSGO algorithm are given as follows.

Improvement 1: First, in a social group, individuals with high similarity tend to gather together to form a niche environment, and people form a complex network through various connections. Second, considering the limitations of individual learning ability, the difficulty of acquiring knowledge, and the diversity of learning methods, when an individual cannot solve complex problems alone, it is easier for individuals to obtain the required knowledge from their nearest neighbors to improve their ability to solve problems. Thus, after weighing the performance and complexity of the algorithm, the dual-population evolutionary algorithm is the best as it enables the two populations to improve their performance through mutual knowledge and talent exchange. The diversified evolution of the two populations ensures diversity, while the exchange of excellent individuals among subpopulations ensures the convergence speed of feasible solutions, realizes complementary advantages, and then improves the performance of the algorithm in solving various complex optimization problems. At the beginning of the DPSGO algorithm, the initial population is randomly divided into population 1 and population 2. In the subsequent evolution process, the two populations use different evolution methods and have information interaction capabilities. Population 2 can enhance the search range of the population by introducing Gaussian mutation and reverse learning. In order to reduce the problem of falling into the local optimum, the evolution strategy adopted by population 2 is to increase the possibility of finding the optimum value by increasing the search range and increasing the diversity of the population. The population evolution method of population 1 is greatly affected by the optimal value within the population, so the local range of contemporary optimal values can be fully searched, which also inherits the characteristics of the original SGO algorithm's strong local searchability. We also realize the information interaction between population 1 and population 2 through the migration operation and the improved "acquiring phase" to prevent population 1 from falling into a local minimum. We will further compare and analyze the search capabilities of the algorithms from the perspectives of accuracy, convergence, and population diversity through simulation experiments in Section IV. Using different evolution strategies can effectively improve the performance of the algorithm, especially if the subpopulation adopts a complementary evolution strategy.

In the improving phase of the DPSGO algorithm, individuals improve their intelligence level by observing the behavior of the optimal individual and learning the advantages of the optimal individual. This evolutionary process comprehensively takes into account human habitual and imitation behaviors. That is, individuals tend to be satisfied with their current behavior or have certain inertia when learning. Thus, while learning and simulating from excellent individuals, individuals will retain some of their own knowledge. We include self-introspection parameters to simulate this behavior. The individual update mode within each group is given as follows:

$$X_{\text{new}_{i,j}} = c \times X_{\text{old}_{i,j}} + r \times (a\text{gbest}_j - X_{\text{old}_{i,j}}) \tag{4}$$

where c is the self-introspection parameter. Its value can be set from 0 to 1, where r is a random number of 0–1, and $a\text{gbest}_j$ is the jth dimension feature number of the current generation optimal individual in the population where the updated individual is located. $X_{\text{old}_{i,j}}$ and $X_{\text{new}_{i,j}}$ are the jth dimension feature numbers before and after the update of individual i, respectively.

In the acquiring phase of the DPSGO algorithm, the interaction of information between subgroups can provide more information for individual learning. The information exchange mechanism between two populations can give individuals a greater chance to jump out of the local extreme in learning, so as to avoid premature algorithm convergence.

The individual update mode within each group is given as follows:

$$\begin{aligned}&\text{if } f(x_i) \text{ is better than } f(x_k)\\&\quad X_{\text{new}_{i,j}} = X_{\text{old}_{i,j}} + r_1 \times (X_{i,j} - X_{k,j}) + r_2 \times (b\text{gbest}_j - X_{i,j})\\&\qquad\qquad + r_3 \times (a\text{gbest}_j - X_{i,j})\\&\text{else}\\&\quad X_{\text{new}_{i,j}} = X_{\text{old}_{i,j}} + r_1 \times (X_{k,j} - X_{i,j}) + r_2 \times (b\text{gbest}_j - X_{i,j})\\&\qquad\qquad + r_3 \times (a\text{gbest}_j - X_{i,j}) \qquad (5)\end{aligned}$$

where r_1, r_2, and r_3 are random numbers between 0 and 1, and X_k is an individual randomly selected from the population where the updated individual is located as the learning object. $a\text{gbest}_j$ is the jth dimension feature number of the current generation optimal individual in the population where the updated individual is located, $b\text{gbest}_j$ is the jth dimension feature number of the optimal individual among all individuals in the two populations of the current generation, and $f(x)$ is the individual fitness evaluation function.

Improvement 2: Considering the deliberative and autonomous learning behaviors of people in actual social groups, especially in collective living, when there is a large difference in the knowledge level among individuals, the inferior individuals will become unsatisfied with their current learning behavior and will consider choosing other learning behaviors. They will make decisions independently according to their own state and perceived information. For example, "self-driven learning" is carried out to explore new knowledge to improve ability levels and narrow the gap with other individuals. We introduce reverse learning technology to simulate this behavior.

Aiming at the weakness of the SGO algorithm in global searchability and its tendency to fall into a local optimal solution, reverse learning technology is introduced to individuals with poor fitness in population 2 to enhance their global searchability. The basic idea is to compare the current solution and the reverse solution. If the reverse solution is better than the current solution, the reverse solution will replace the current solution. Reverse learning technology can quickly expand the search space, enrich the population's diversity, has a better ability to explore unknown solutions, and increase the possibility of finding the global optimal solution and jumping out of the local optimal solution. It has been reported that the reverse solution is closer to the optimal solution than the current solution, and the probability is almost 50% using this technique [37]. Suppose that $X = [x_1, x_2, \ldots, x_D]$ is a point in D-dimensional space, where $x_i \in [a_i, b_i]$, $i = 1, 2, \ldots, D$. The reverse solution of X is $X^* = [x_1^*, x_2^*, \ldots, x_D^*]$, and the calculation formula of the reverse solution is given as follows:

$$x_i^* = a_i + b_i - x_i. \qquad (6)$$

Improvement 3: The migration behavior existing in real human social groups, even under significant geographical constraints, can realize the exchange of individuals and information via the rapidly developing transportation and communication networks. To account for this migration operation between elite individuals, we introduce the elite mechanism of survival of the fittest for the receiving population. Migration operation is the basic operator in the biogeographic optimization algorithm, where a migration operator realizes the transfer of information and knowledge between different solutions. Through migration operation, individuals with poor knowledge levels can obtain the characteristics of better individuals and improve their knowledge level. We introduce an immigration operation between the two populations, where population 2 has strong global searchability, and population 1 has strong local searchability. The optimal individuals in population 2 immigrate into population 1, and the individuals with the highest survival of the fittest mechanisms are adopted to replace the individuals with the worst fitness in population 1. This increases the diversity of individuals within population 1 to prevent it from falling into the local optimal solution.

Improvement 4: In actual human social groups, excellent individuals have stronger knowledge reserve and self-learning abilities. However, in the standard SGO algorithm, the optimal individuals in the population lack self-learning and improvement. Using the Gaussian mutation operation on the optimal individual enhances their ability to explore a better solution, ensuring that the optimal individual of the population retains a better solution every time it performs Gaussian mutation. This operation simulates the behavior of the optimal individual self-learning and improving ability. In order to solve the problem of falling into local optimal solution, the Gaussian mutation operator is introduced. Compared with other mutation operators, the Gaussian mutation operator has the highest probability of mutation near the mean value, which makes the development of the algorithm more effective. Population 2 produces a large number of Gaussian mutation individuals near the current optimal value, which are replaced according to the fitness value. By introducing Gaussian variation, the search range of the optimal value is increased, and the searchability is improved. The Gaussian mutation operation is given as follows:

$$X_{G,j} = X_{i,j} + c_j \times N(0, 1) \qquad (7)$$

where $X_{G,j}$ is the jth dimensional value of the Gaussian variant individual, $X_{i,j}$ is the jth dimensional value of the contemporary optimal individual, and $N(0, 1)$ is a normal Gaussian distributed random variable with a mean of 0 and a variance of 1. c_j is the variation step size of the jth dimensional, and $j = 1, 2, \ldots, D$. The flowchart of the DPSGO algorithm is shown in Fig. 1.

IV. Validation of DPSGO Algorithm for Processing Multispectral Temperature Measurement Data

This section will study the root causes of the social hot issue of aviation safety. Through theoretical simulation and experiments, it will verify the effectiveness of using the DPSGO algorithm to process the multispectral temperature measurement data of aeroengine turbine blades and use the temperature to monitor the operation safety of aeroengine, so as to reduce people's concerns about aviation safety. Aviation, like a spanning activity and process of human society

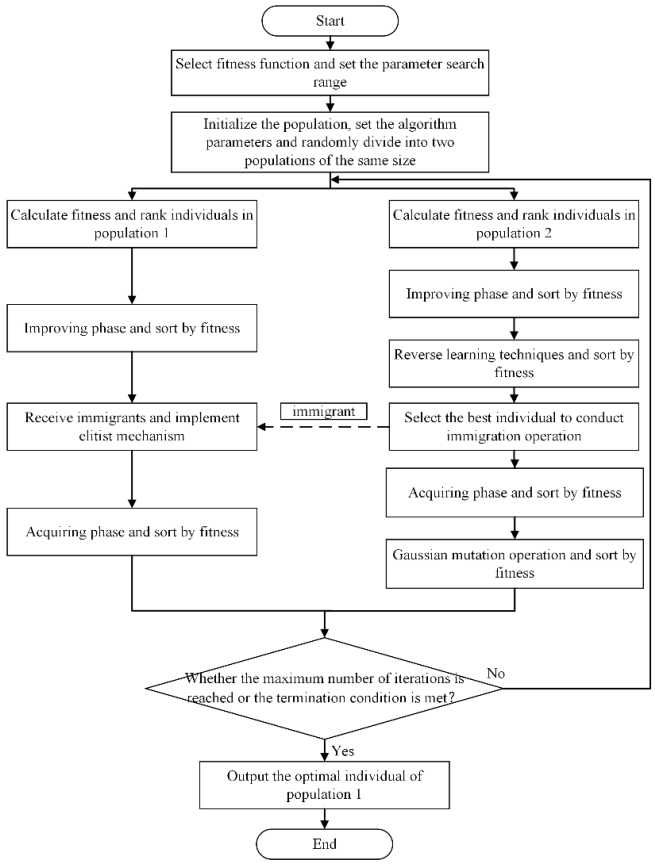

Fig. 1. Flowchart of the DPSGO algorithm.

to social space, plays a positive role in national and regional economic development, but, at the same time, some people are worried about aviation safety, and it has become a social hot issue. Although the development trend of aviation accidents is decreasing and the probability of accident occurrence is small, the death rate of aircraft accidents is quite high. Every "point hair" air crash around the world will bring great harm to many families [38], [39]. The aeroengine is the aircraft's power plant, where the turbine is the main hot end component of the engine. Turbine blades are prone to failure when working in a high-temperature and high-pressure environment for a long time. Accurately measuring the temperature of the turbine blades can monitor and evaluate the working status of the blades, which is of great significance to ensure the safe operation of the engine. The engine turbine stage profile and rotor blade model are shown in Fig. 2.

A. Basic Principle of Multispectral Radiation Thermometry

Planck's law is the basic law of thermal radiation. It describes the relationship between blackbody radiation and temperature and wavelength, which can be expressed as follows:

$$M(\lambda, T) = c_1 \lambda^{-5} (e^{c_2/\lambda T} - 1)^{-1} \tag{8}$$

where $c_1 = 3.7418 \times 10^{-16}$ W $\cdot$ m is the first Planck coefficient and $c_2 = 1.4388 \times 10^{-2}$ m $\cdot$ K is the second Planck coefficient. λ is the measured wavelength, and $M(\lambda, T)$ is the radiation emissivity when the target temperature is T and the wavelength is λ.

Due to the reflected radiation in the high-temperature background environment and the emissivity on the surface of the object to be measured, the radiation received by the radiation pyrometer can be expressed as follows:

$$M(\lambda, T) = \varepsilon_\lambda M(\lambda, T_\mathrm{b}) + (1 - \varepsilon_\lambda) M(\lambda, T_\mathrm{r}) \tag{9}$$

where T is the measurement temperature of the radiation pyrometer, T_b is the target blackbody temperature, T_r is the ambient temperature, $M(\lambda, T)$ is the total radiation emission received by the detector, $M(\lambda, T_\mathrm{b})$ is the radiation emissivity of the blackbody of the target, and $M(\lambda, T_\mathrm{r})$ is the amount of radiation from the high-temperature environment to the surface of the measured object. ε_λ is the emissivity of the measured object surface, and the value of $(1-\varepsilon_\lambda)$ is equal to the surface reflectivity of an opaque object.

The emissivity is the ratio of the heat energy radiated by the object at a certain temperature to the radiation energy of the blackbody at the same temperature. The emissivity value is related to the temperature, wavelength, surface state, and other factors of the object. Several commonly used emissivity models are given as follows:

$$\varepsilon(\lambda, T) = a + b\lambda \tag{10}$$

$$\varepsilon(\lambda, T) = e^{a+b\lambda} \tag{11}$$

$$\varepsilon(\lambda, T) = \frac{1}{2} + \frac{1}{2}\sin(a\lambda + b) \tag{12}$$

$$\varepsilon(\lambda, T) = a\lambda^2 + b\lambda + c. \tag{13}$$

For the multiwavelength pyrometer with n channels, the radiation received by each channel is given as follows:

$$\begin{cases} M(\lambda_1, T_\mathrm{b}) = \dfrac{M(\lambda_1, T_m) - (1-\varepsilon_1) M(\lambda_1, T_\mathrm{r})}{\varepsilon_1} \\ M(\lambda_2, T_\mathrm{b}) = \dfrac{M(\lambda_2, T_m) - (1-\varepsilon_2) M(\lambda_2, T_\mathrm{r})}{\varepsilon_2} \\ \cdots \\ M(\lambda_n, T_\mathrm{b}) = \dfrac{M(\lambda_n, T_m) - (1-\varepsilon_n) M(\lambda_n, T_\mathrm{r})}{\varepsilon_n}. \end{cases} \tag{14}$$

Equation (14) is the implicit function equation group between the emissivity coefficient and the target true temperature. However, as it is difficult to solve (14) directly, it can be transformed into an optimization problem to solve emissivity model coefficients and real temperature. The objective equation is given as follows:

$$\begin{cases} \Delta = \min \displaystyle\sum_{i=1}^{n} \big[M(\lambda_i, T_m) - (1-\varepsilon_{\lambda_i}) M(\lambda_i, T_\mathrm{r}) \\ \qquad\qquad - \varepsilon_{\lambda_i} M(\lambda_i, T) \big]^2 \\ \varepsilon_{\lambda_i} = f(\lambda, T) \\ 0 \le \varepsilon_{\lambda_i} \le 1 \end{cases} \tag{15}$$

where ε_{λ_i} is the emissivity calculated by the emissivity model at the wavelength of the ith channel, $f(\lambda, T)$ is the selected emissivity model, T is the true surface temperature of an unknown object, and T_r is the temperature of the object around which there is reflected radiation.

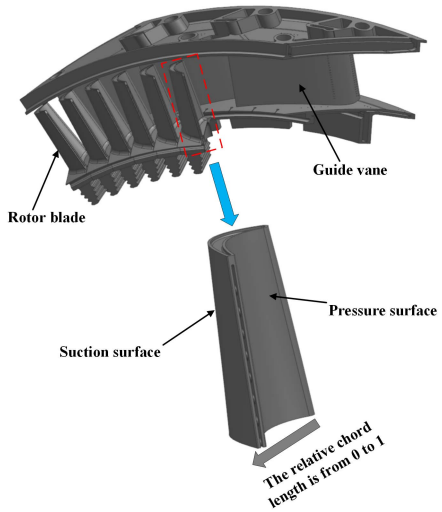

Fig. 2. Engine turbine stage profile and rotor blade model.

B. Performance Test of DPSGO Algorithm

To test the performance of the DPSGO and SGO algorithms in processing multispectral temperature measurement data, simulation experiments were set as follows. The temperature to be measured was assumed to be 600 °C, the background temperature was assumed to be 800 °C, and the simulated wavelengths were selected to be 1.3, 1.5, 1.5, 1.6, 1.7, and 1.8 μm, respectively. The emissivity model was assumed to be $\varepsilon(\lambda, T) = 0.5 + 0.5\sin(0.7\lambda - 0.7)$, as shown in (12). Under this condition, the search range of the two parameters of the emissivity model was set to $0.3 \le a \le 1.1$, $-1.1 \le b \le -0.3$, and the temperature search range was set to 550 °C $\le T \le$ 650 °C. The initial population and iteration times of the two algorithms were the same, where the population size of the two algorithms was 100 and the maximum iteration time was 100. The self-introspection parameters of population 1 and population 2 of the DPSGO algorithm were set as 0.2 and 0.15, respectively, the Gaussian variable step size was $c_1 = c_2 = 0.1$, $c_3 = 5$, and the reverse learning ratio was 0.2. The self-introspection parameter of the SGO algorithm was 0.2. The DPSGO algorithm and the SGO algorithm were used to repeat the calculation 100 times, respectively. The temperature calculation results are shown in Fig. 3, which reflects the accuracy and stability of the two algorithms. The lowest temperature calculated by the DPSGO algorithm is 599.7749 °C, the highest temperature is 600.1171 °C, the maximum error is 0.1171 °C, and the average temperature error is 0.0358 °C. The lowest temperature calculated by the SGO algorithm is 599.2304 °C, the highest temperature is 601.105 °C, the maximum error is 1.105 °C, and the average temperature error is 0.1775 °C. From the perspective of stability, the mean square deviation of the DPSGO algorithm for the single temperature solution is 0.0014, and the mean square deviation of the SGO algorithm for the single temperature solution is 0.0446. Therefore, DPSGO has better accuracy and stability than the SGO algorithm.

The iterative curves of the two algorithms are shown in Fig. 4, which illustrates that, under the same conditions, the DPSGO algorithm tends to converge after 30 iterations, while the SGO algorithm tends to converge after 50 iterations. Fig. 4(a) shows that the fitness of the DPSGO algorithm converges faster, and Fig. 4(b) shows that, after the algorithm converges, the temperature iteration curve will no longer produce fluctuations to reach a stable value. Combined with the accuracy, it can be determined that the convergence of DPSGO is better than the SGO algorithm.

In order to measure the diversity of the population, the normalized average distance between different individuals in the population is introduced as a measurement index. The calculation method is shown in the following equations:

$$D(X_m, X_n) = \sqrt{\sum_{j=1}^{D}(X_{mj} - X_{nj})^2} \tag{16}$$

$$D^*(X_m, X_n) = \frac{D(X_m, X_n)}{\max(D(X_m, X_n))} \tag{17}$$

$$\overline{D} = \frac{2\sum_{m=1}^{N-1}\sum_{n=m+1}^{N} D^*(X_m, X_n)}{N(N-1)} \tag{18}$$

where $m = 1, 2, \ldots, N-1$, $n = m+1, \ldots, N$, N is the number of populations, m and n represent different individuals, and $j = 1, 2, \ldots, D$ represents the characteristic dimension. $D(X_m, X_n)$ is the distance between different individuals, $D^*(X_m, X_n)$ is the normalized distance between different individuals, and $\overline{D}$ is the normalized average distance of all individuals in the population.

The comparison of population diversity between the two algorithms is shown in Fig. 5. Fig. 5(a) shows the comparison of the population diversity of all individuals of the two algorithms. It can be seen that the population diversity of the SGO algorithm decreases rapidly and is low. Due to the single evolutionary form, the SGO algorithm is easy to falls into local optimal value. However, the DPSGO algorithm uses a variety of improved evolution methods, so the overall population diversity is higher than the SGO algorithm, which means that it has the opportunity to comprehensively search for a wider space. Fig. 5(b) shows the comparison of population diversity between population 1 and population 2 of the DPSGO algorithm. It can be seen that, because population 2 adopts a variety of evolution methods, the population diversity has been maintained at a high level in the early stage and declined slowly, and the search range is also wider. By continuously receiving the best immigrant individuals from population 2 and adopting optimized evolution strategies, although the population diversity of population 1 is lower than that of population 2, it still produces greater volatility. The greater the population diversity, the more scattered the individuals of the population, which is more conducive to the global search of the algorithm. Conversely, the more concentrated the population individuals are, the more conducive to the local search and convergence of the algorithm. The population diversity of the DPSGO algorithm decreases slowly in the early stage and has a larger vibration frequency and amplitude, so a better balance can be found in the global search and the local search. Comprehensive calculation accuracy, convergence, and population diversity prove that the DPSGO algorithm is more effective and efficient than the SGO algorithm.

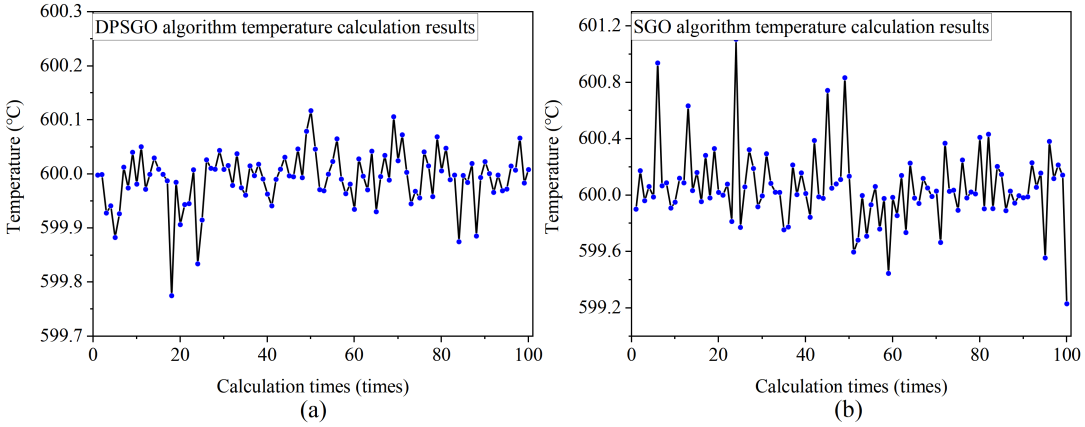

Fig. 3. Temperature calculation results of the two algorithms: (a) DPSGO algorithm temperature calculation results and (b) SGO algorithm temperature calculation results.

C. Theoretical Simulation Verification of DPSGO Algorithm Processing Multispectral Radiation Temperature Measurement Data

Before processing the multispectral radiation temperature measurement data, the discrete model of turbine blades is established to obtain the relevant information of reflected radiation. The analysis process of the reflected radiation model mainly includes the following steps. First, the discrete model of the turbine blades is established, and the points of the rotor blade to be measured are selected. The front stage guide vanes and front stage rotor blades facets are "visualized" to select the facets that may transfer heat radiation to the points to be measured without considering the mutual occlusion. Second, the occlusion between the blades is judged, and the blades with mutual occlusion are deleted. Finally, the radiation from the surrounding environment to the point to be measured can be obtained by calculating the angle coefficient combined with the blade temperature distribution, and the reflected radiation from the surface of the point to be measured can be obtained when the emissivity is known. An example of the analysis process of the reflected radiation model is shown in Fig. 6.

The temperature distribution of guide vanes and rotor blades was set according to the proposed analysis model of reflected radiation. The temperature error caused by the reflected radiation was calculated when the blade span heights were 25%, 50%, and 75%, respectively, and the relative chord length was 0–1. During the simulation analysis, the temperature distribution of the guide vanes was set at 450 °C–980 °C, and the temperature of the rotor blade is set at 560 °C. The wavelengths are set to 1.3, 1.4, 1.5, 1.6, 1.7, and 1.8 μm, and the emissivity at each wavelength was selected as 0.6, 0.62, 0.67, 0.7, 0.75, and 0.78, according to the previous measured data. We employed the non-dominant sorting genetic algorithm-II (NSGA-II) and improved non-dominant sorting genetic algorithm-II (INSGA-II) algorithms for simulation comparison, which are commonly used for processing radiation temperature measurement data [40]. The emissivity model was selected as a sinusoidal model. The initial population size and search range of the four types of algorithms were the same, where the population size was 100,

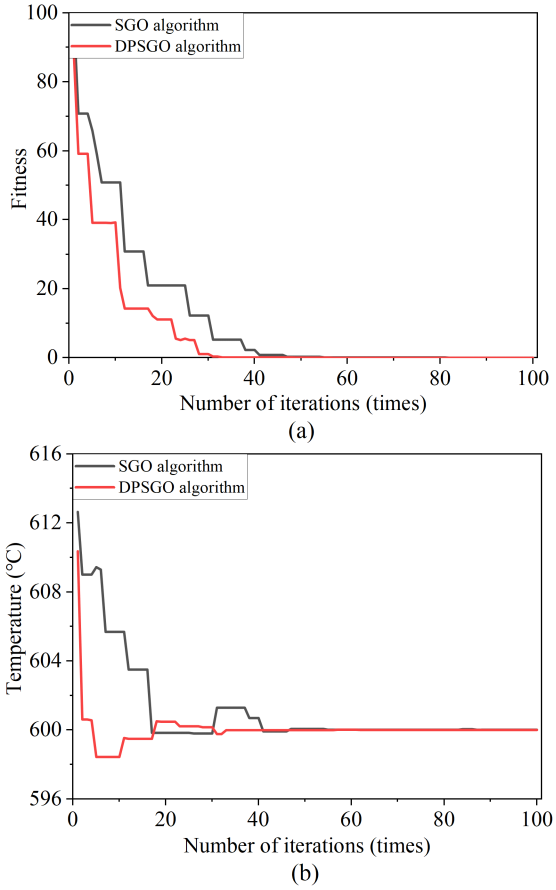

Fig. 4. Iteration curves of the DPSGO and SGO algorithms: (a) fitness iteration curve and (b) temperature iteration curve.

and the number of iterations was 50. The selection of the DPSGO and SGO parameters is the same as above. The crossover rate of the NSGA-II and INSGA-II algorithms was 0.78, and the mutation rate was 0.15. The cluster number of the INSGA-II algorithm was 12, and the individual proportion of calculated symmetric solutions was 0.2. The three groups of blade span height temperature errors caused by reflected

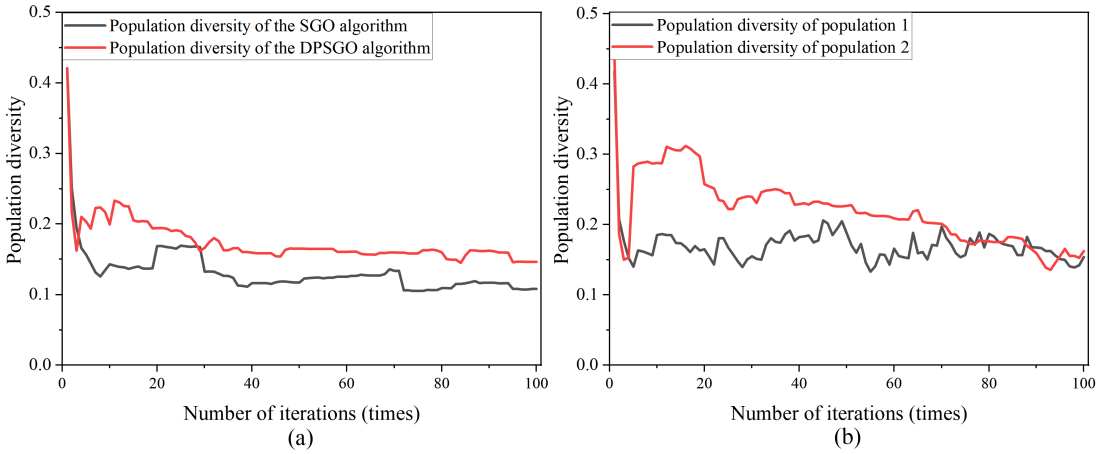

Fig. 5. Comparison of population diversity between the DPSGO algorithm and SGO algorithm: (a) comparison of the population diversity of all individuals of the two algorithms and (b) comparison of population diversity between population 1 and population 2 of the DPSGO algorithm.

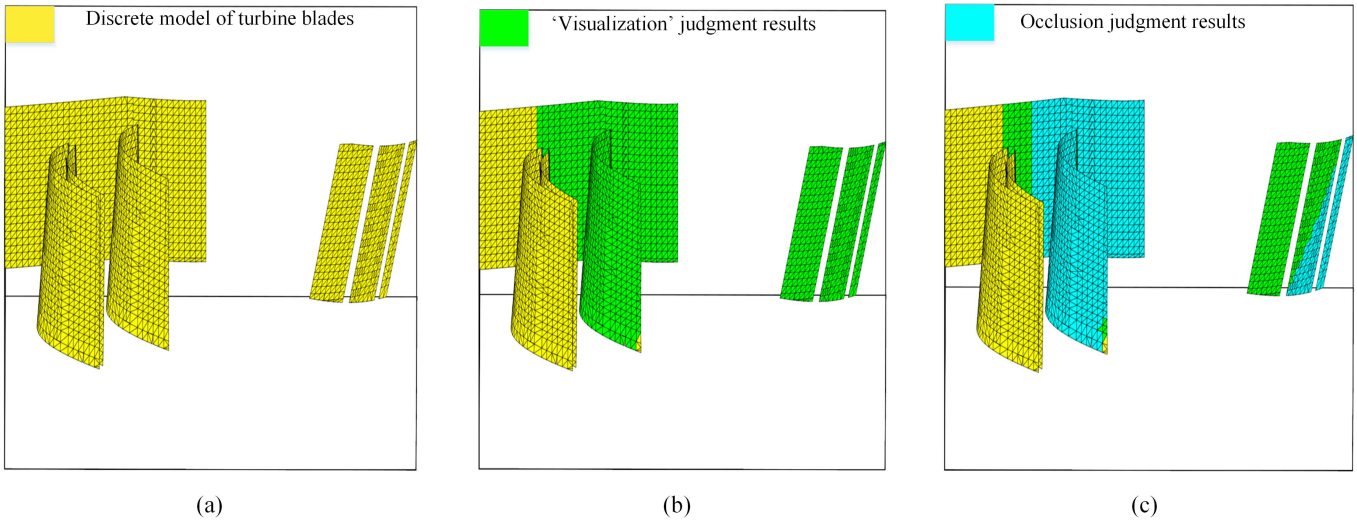

Fig. 6. Diagram of reflected radiation analysis model process: (a) discrete model of turbine blades; (b) visualization judgment results; and (c) final result after occlusion judgment.

radiation are obtained, as shown in Fig. 7(a). Fig. 7(b) shows the temperature error after processing the multispectral radiation temperature measurement data using the DPSGO algorithm. The maximum temperature error is 3.0832 °C, and the average temperature error is 1.1411 °C. Fig. 7(c) shows the temperature error after processing the multispectral radiation temperature measurement data using the SGO algorithm. The maximum temperature error is 6.8992 °C, and the average temperature error is 1.7952 °C. Fig. 7(d) shows the temperature error after processing the multispectral radiation temperature measurement data using the NSGA-II algorithm. The maximum temperature error is 6.7642 °C, and the average temperature error is 1.529 °C. Fig. 7(e) shows the temperature error after processing the multispectral radiation temperature measurement data using the INSGA-II algorithm. The maximum temperature error is 5.18 °C, and the average temperature error is 1.2756 °C. By comparing the calculation results of the various algorithms, the effectiveness of using the DPSGO algorithm to process multispectral radiation temperature measurement data is verified.

D. Experimental Verification of DPSGO Algorithm for Processing Actual Multispectral Radiation Temperature Measurement Data

The sample to be tested was placed in a constant temperature furnace, and its surface temperature was changed by setting a cooling chamber and introducing cold air. The total radiation on the surface of the sample was recorded using a high-temperature radiometer. The radiation from the high-temperature background to the sample to be tested was known by previous analysis, and a thermocouple was used to determine the real surface temperature of the sample. The constant temperature of the constant temperature furnace was 690 °C, and the data of 35 groups of samples were collected. In this experiment, the multispectral radiation data

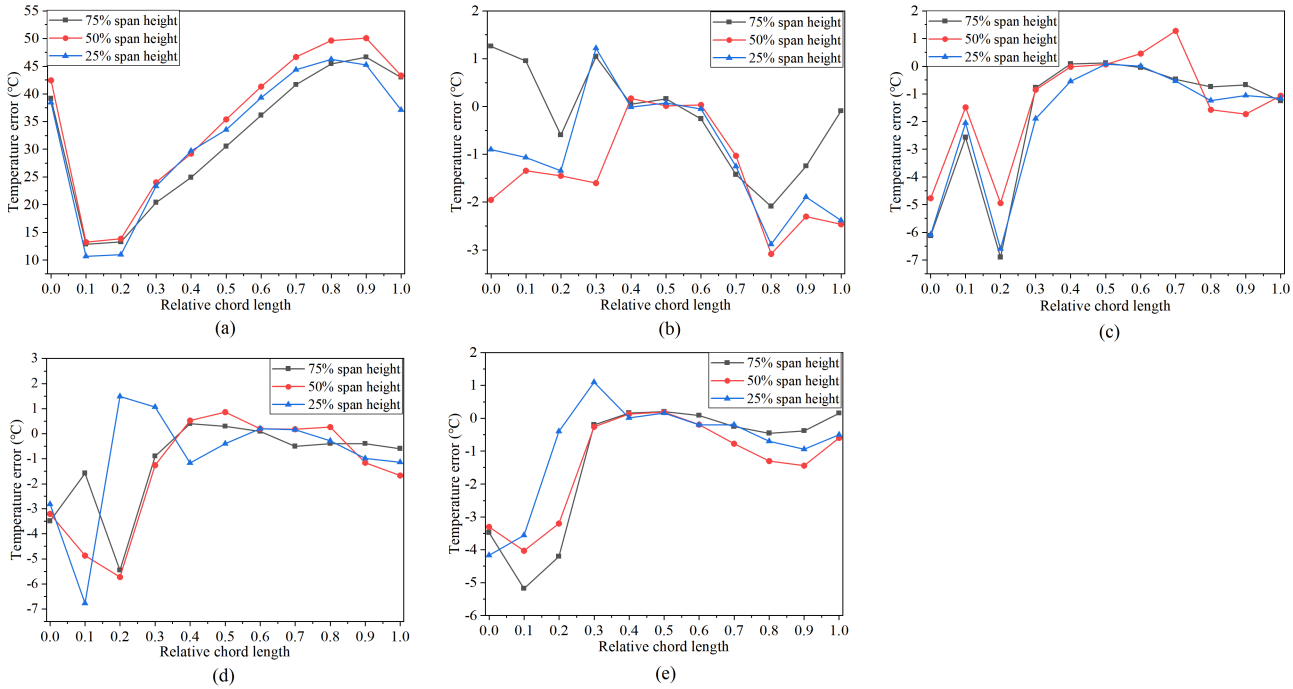

Fig. 7. Temperature error: (a) temperature error caused by reflected radiation; (b) temperature error after DPSGO algorithm processing; (c) temperature error after SGO algorithm processing; (d) temperature error after NSGA-II algorithm processing; and (e) temperature error after INSGA-II algorithm processing.

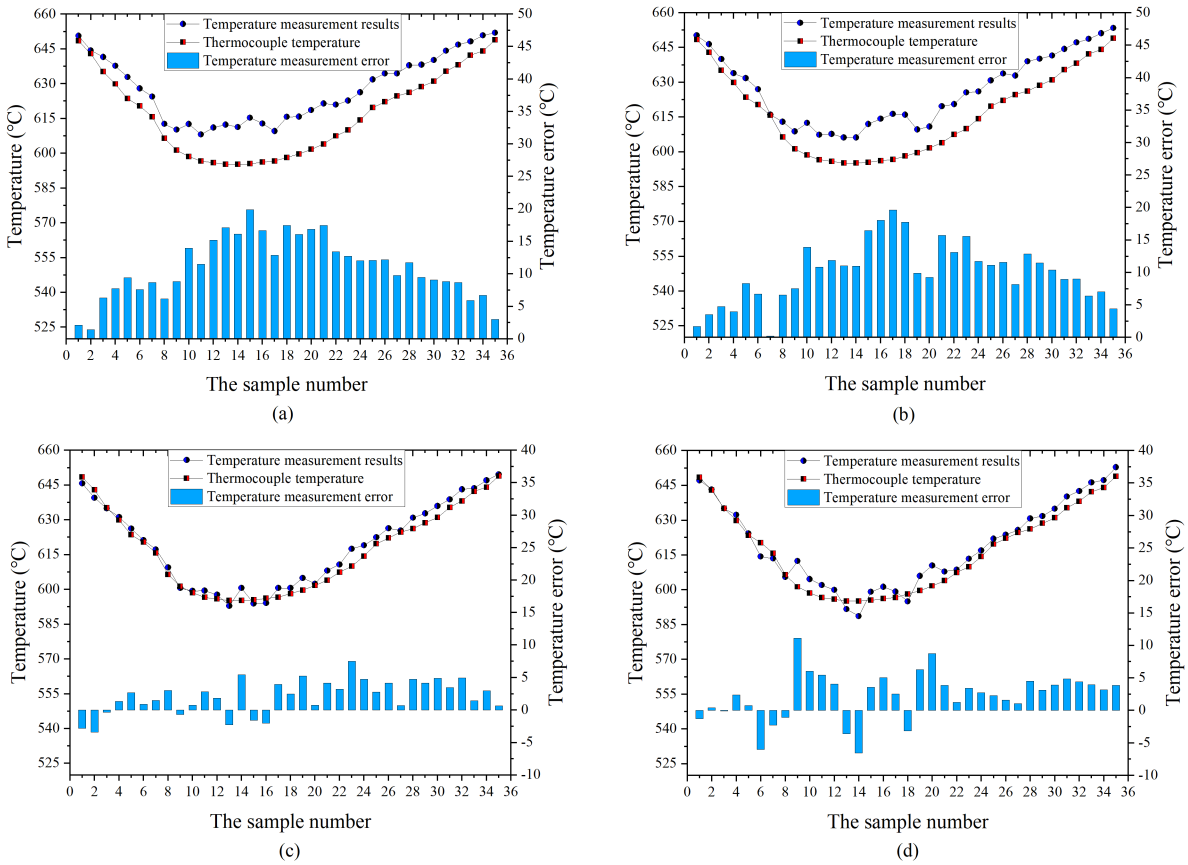

Fig. 8. Experimental results: (a) experimental results of DPSGO algorithm under linear emissivity model (increase); (b) experimental results of the DPSGO algorithm under exponential emissivity model (increase); (c) experimental results of the DPSGO algorithm under sinusoidal emissivity model; and (d) experimental results of the original SGO algorithm under sinusoidal emissivity model.

selection is 1.3, 1.4, 1.5, 1.6, 1.7, and 1.8 μm, with a bandwidth of 0.02 μm. Three types of emissivity models were selected: the linear emissivity model (increase), exponential emissivity model (increase), and sinusoidal emissivity model [refer to (10)–(12)]. Finally, the temperature measurement error was calculated according to the results of the algorithm and the thermocouple indication. With the exception of the population size and search range, the DPSGO and SGO algorithm parameters were the same as the above simulation parameters. The population size was 100, and the number of iterations was 100. The search range of the two parameters of the emissivity model was set to $-0.1 \leq a \leq 0.9$, $-0.1 \leq b \leq 0.9$, and the temperature search range was set to 570 °C $\leq T \leq$ 670 °C.

According to the above experimental settings, three commonly used emissivity models were selected for calculation, and the radiation temperature measurement data were processed by using the DPSGO algorithm to obtain the measurement temperature and its error. The experimental results are shown in Fig. 8(a)–(c). By comparing the experimental results of the three emissivity models, it can be concluded that, under the condition of the sinusoidal emissivity model, the DPSGO algorithm has the best results, and the sinusoidal emissivity model is more suitable for the experimental data. As shown in Fig. 8(c), the maximum temperature measurement error is less than 7.5 °C, while the temperature measurement errors of other emissivity models are larger, even reaching up to 19.8 °C.

Under the same experimental conditions and emissivity model, the temperature measurement results of the DPSGO and the original SGO algorithms are then compared. The temperature measurement results and errors of the DPSGO algorithm are shown in Fig. 8(c), and the temperature measurement results and errors of the original SGO algorithm are shown in Fig. 8(d). The maximum temperature error in the temperature measurement results calculated by the DPSOG algorithm is 7.5 °C, and the average error temperature is 2.9 °C. In the temperature measurement results calculated by the SGO algorithm, the maximum temperature error is 11.1 °C, and the average error temperature is 3.7 °C. Experimental results show that it is effective to use the DPSGO algorithm combined with reflected radiation correction to process aeroengine multispectral radiation temperature measurement data.

V. Conclusion

In this article, a DPSGO algorithm was proposed based on the behavior law of the actual human social groups. The performance of the DPSGO algorithm was compared with a variety of swarm intelligence algorithms and simulation experiments demonstrated that the algorithm has a better performance. Aiming at the socially hot issue of aviation safety, the effectiveness of using the DPSGO algorithm to process aeroengine multispectral radiation temperature measurement data was verified by theoretical simulation and experiments. The simulation and experimental results demonstrated that the use of the DPSGO algorithm combined with reflected radiation correction to process aeroengine multispectral radiation temperature measurement data could reduce the temperature measurement error to within 7.5 °C. This article is of great significance to the design and optimization of swarm intelligence algorithms by using the behavior law of human social groups and provides valuable guidance for enhancing the safety monitoring of aeroengines.

References

[1] A.-F. Attia, M. A. Elaziz, A. E. Hassanien, and R. A. El-Sehiemy, "Prediction of solar activity using hybrid artificial bee colony with neighborhood rough sets," *IEEE Trans. Comput. Social Syst.*, vol. 7, no. 5, pp. 1123–1130, Oct. 2020.

[2] A. H. Khan, X. Cao, S. Li, and C. Luo, "Using social behavior of beetles to establish a computational model for operational management," *IEEE Trans. Comput. Social Syst.*, vol. 7, no. 2, pp. 492–502, Apr. 2020.

[3] M. Dorigo and G. D. Caro, "Ant colony optimization: A new metaheuristic," in *Proc. Congr. Evol. Comput.*, vol. 2, Jul. 1999, pp. 1470–1477.

[4] X.-S. Yang, "Firefly algorithms for multimodal optimization," in *Proc. Int. Symp. Stochastic Algorithms*. Berlin, Germany: Springer, 2009, pp. 169–178.

[5] X.-S. Yang, "A new metaheuristic bat-inspired algorithm," in *Nature Inspired Cooperative Strategies for Optimization (NICSO 2010)*. Berlin, Germany: Springer, 2010, pp. 65–74.

[6] E. Demirci and A. R. Yıldız, "A new hybrid approach for reliability-based design optimization of structural components," *Mater. Test.*, vol. 61, no. 2, pp. 111–119, Feb. 2019.

[7] Z. Meng, G. Li, X. Wang, S. M. Sait, and A. R. Yıldız, "A comparative study of Metaheuristic algorithms for reliability-based design optimization problems," *Arch. Comput. Methods Eng.*, vol. 28, no. 3, pp. 1853–1869, May 2021.

[8] G. Dhiman *et al.*, "EMoSOA: A new evolutionary multi-objective seagull optimization algorithm for global optimization," *Int. J. Mach. Learn. Cybern.*, vol. 12, no. 2, pp. 571–596, Feb. 2021.

[9] P. Champasak, N. Panagant, N. Pholdee, S. Bureerat, and A. R. Yildiz, "Self-adaptive many-objective meta-heuristic based on decomposition for many-objective conceptual design of a fixed wing unmanned aerial vehicle," *Aerosp. Sci. Technol.*, vol. 100, May 2020, Art. no. 105783.

[10] G. Dhiman, M. Garg, A. Nagar, V. Kumar, and M. Dehghani, "A novel algorithm for global optimization: Rat swarm optimizer," *J. Ambient Intell. Humanized Comput.*, vol. 12, no. 8, pp. 8457–8482, Aug. 2021.

[11] M. A. Elaziz *et al.*, "An improved marine predators algorithm with fuzzy entropy for multi-level thresholding: Real world example of COVID-19 CT image segmentation," *IEEE Access*, vol. 8, pp. 125306–125330, 2020.

[12] H. Zhu, "Computational social simulation with E-CARGO: Comparison between collectivism and individualism," *IEEE Trans. Comput. Social Syst.*, vol. 7, no. 6, pp. 1345–1357, Dec. 2020.

[13] H. Khalil and G. Wainer, "Cell-DEVS for social phenomena modeling," *IEEE Trans. Comput. Social Syst.*, vol. 7, no. 3, pp. 725–740, Jun. 2020.

[14] Z. Z. Liu, D. H. Chu, C. Song, X. Xue, and B. Y. Lu, "Social learning optimization (SLO) algorithm paradigm and its application in QoS-aware cloud service composition," *Inf. Sci.*, vol. 326, pp. 315–333, Jan. 2016.

[15] X.-F. Xie, W.-J. Zhang, and Z.-L. Yang, "Social cognitive optimization for nonlinear programming problems," in *Proc. Internat. Conf. Mach. Learn. Cybern.*, vol. 2, 2002, pp. 779–783.

[16] J. Z. Sun, G. H. Geng, H. Chen, and M. Q. Zhou, "An improved social cognitive optimization algorithm," *Appl. Mech. Mater.*, vols. 427–429, pp. 2580–2583, Sep. 2013.

[17] Y. Gong, J. Zhang, and Y. Li, "From the social learning theory to a social learning algorithm for global optimization," in *Proc. IEEE Int. Conf. Syst. Man Cybern.*, Oct. 2014, pp. 222–227.

[18] X. Lin, J. Wu, J. Li, X. Zheng, and G. Li, "Friend-as-learner: Socially-driven trustworthy and efficient wireless federated edge learning," *IEEE Trans. Mobile Comput.*, early access, Apr. 21, 2021, doi: 10.1109/TMC.2021.3074816.

[19] J. Cao *et al.*, "Local experts finding using user comments in location-based social networks," *Trans. Emerg. Telecommun. Technol.*, vol. 30, no. 9, p. 18, Sep. 2019.

[20] A. Naik, S. C. Satapathy, A. S. Ashour, and N. Dey, "Social group optimization for global optimization of multimodal functions and data clustering problems," *Neural Comput. Appl.*, vol. 30, no. 1, pp. 271–287, Jul. 2018.

[21] N. Dey, V. Rajinikanth, A. S. Ashour, and J. M. R. S. Tavares, "Social group optimization supported segmentation and evaluation of skin melanoma images," *Symmetry*, vol. 10, no. 2, p. 51, 2018.

[22] V. Rajinikanth and S. C. Satapathy, "Segmentation of ischemic stroke lesion in brain MRI based on social group optimization and fuzzy-tsallis entropy," *Arabian J. Sci. Eng.*, vol. 43, no. 8, pp. 4365–4378, Aug. 2018.

[23] V. Rajinikanth, S. C. Satapathy, N. Dey, and R. Vijayarajan, "DWT-PCA image fusion technique to improve segmentation accuracy in brain tumor analysis," in *Microelectronics, Electromagnetics and Telecommunications*. Singapore: Springer, 2018, pp. 453–462.

[24] S. P. Praveen, K. T. Rao, and B. Janakiramaiah, "Effective allocation of resources and task scheduling in cloud environment using social group optimization," *Arabian J. Sci. Eng.*, vol. 43, no. 8, pp. 4265–4272, Aug. 2018.

[25] N. Kalla and P. Parwekar, "Social group optimization (SGO) for clustering in wireless sensor networks," in *Intelligent Engineering Informatics*, vol. 695. Singapore: Springer, 2018, pp. 119–128. [Online]. Available: https://link.springer.com/chapter/10.1007%2F978-981-10-7566-7_13#citeas, doi: 10.1007/978-981-10-7566-7_13.

[26] V. S. Chakravarthy, P. S. R. Chowdary, S. C. Satpathy, S. K. Terlapu, and J. Anguera, "Antenna array synthesis using social group optimization," in *Microelectronics, Electromagnetics and Telecommunications*. Singapore: Springer, 2018, pp. 895–905.

[27] B. Janakiramaiah, G. Kalyani, S. Chittineni, and B. N. K. Rao, "An unbiased privacy sustaining approach based on SGO for distortion of data sets to shield the sensitive patterns in trading alliances," in *Smart Intelligent Computing and Applications*. Singapore: Springer, 2019, pp. 165–177.

[28] N. Cheke, J. Chandra, and S. K. Dandapat, "Understanding the impact of geographical distance on online discussions," *IEEE Trans. Comput. Social Syst.*, vol. 7, no. 4, pp. 858–872, Aug. 2020.

[29] C.-T. Li and S.-D. Lin, "Social flocks: Simulating crowds to discover the connection between spatial-temporal movements of people and social structure," *IEEE Trans. Comput. Social Syst.*, vol. 5, no. 1, pp. 33–45, Mar. 2018.

[30] H. Lu *et al.*, "Social signal-driven knowledge automation: A focus on social transportation," *IEEE Trans. Comput. Social Syst.*, vol. 8, no. 3, pp. 737–753, Jun. 2021.

[31] S.-S. Zhang, X. Liang, Y.-D. Wei, and X. Zhang, "On structural features, user social behavior, and kinship discrimination in communication social networks," *IEEE Trans. Comput. Social Syst.*, vol. 7, no. 2, pp. 425–436, Apr. 2020.

[32] I. Annamoradnejad, M. Fazli, J. Habibi, and S. Tavakoli, "Cross-cultural studies using social networks data," *IEEE Trans. Comput. Social Syst.*, vol. 6, no. 4, pp. 627–636, Aug. 2019.

[33] W. Jiang, S. Lv, Y. Wang, J. Chen, X. Liu, and Y. Sun, "Computational experimental study on social organization behavior prediction problems," *IEEE Trans. Comput. Social Syst.*, vol. 8, no. 1, pp. 148–160, Feb. 2021.

[34] X. Wei, G. Xu, H. Wang, Y. He, Z. Han, and W. Wang, "Sensing users' emotional intelligence in social networks," *IEEE Trans. Comput. Social Syst.*, vol. 7, no. 1, pp. 103–112, Feb. 2020.

[35] S. Satapathy and A. Naik, "Social group optimization (SGO): A new population evolutionary optimization technique," *Complex Intel. Syst.*, vol. 2, no. 3, pp. 173–203, 2016.

[36] C. Census, H. Wang, J. Zhang, P. Deng, and T. Li, "Particle subswarms collaborative clustering," *IEEE Trans. Comput. Social Syst.*, vol. 6, no. 6, pp. 1165–1179, Dec. 2019.

[37] H. R. Tizhoosh, "Opposition-based learning: A new scheme for machine intelligence," in *Proc. Int. Conf. Comput. Intell. Modeling, Control Autom. Int. Conf. Intell. Agents, Web Technol. Internet Commerce (CIMCA-IAWTIC)*, Nov. 2005, pp. 695–701.

[38] IATA. (2019). *LOC-I Accident Analysis Report*. Accessed: Jul. 9, 2021. [Online]. Available: https://www.iata.org/contentassets/b6eb2adc248c484192101edd1ed36015/loc-i_2019.pdf

[39] D. Kelly and M. Efthymiou, "An analysis of human factors in fifty controlled flight into terrain aviation accidents from 2007 to 2017," *J. Saf. Res.*, vol. 69, pp. 155–165, Jun. 2019.

[40] L. Chen *et al.*, "Multi-spectral temperature measurement based on adaptive emissivity model under high temperature background," *Infr. Phys. Technol.*, vol. 111, Dec. 2020, Art. no. 103523.

Chao Wang received the B.S. degree in mechanical engineering and the M.S. degree in mechanical materials processing from Tsinghua University, Beijing, China, in 2000 and 2003, respectively, and the Ph.D. degree in material science from the University of Oxford, Oxford, U.K., in 2008.

Since 2012, he has been a Professor with the University of Electronic Science and Technology of China, Chengdu, China. He has applied for 110 domestic and foreign invention patents, of which five U.S. patents and more than 50 Chinese invention patents have been authorized. He has authored more than 70 SCI search articles. His research interests include *in situ* multiparameters measurement instruments for semiconductor epitaxial growth, *in situ* temperature measurement instruments for aeroengine turbine blades, and energy conversion materials and devices.

Xianqi Zhang was born in Harbin, China, in 1998. He is currently pursuing the master's degree with the College of Information and Communication Engineering, Harbin Engineering University, Harbin.

Yi Niu received the B.S. degree in environmental engineering from Sichuan Normal University, Chengdu, China, in 2015, and the Ph.D. degree in materials science and engineering from the University of Science and Technology of China, Chengdu, in 2020.

Since 2021, she has been an Associate Researcher with the University of Electronic Science and Technology of China, Chengdu. She has authored more than ten peer-reviewed journal articles in high-impact journals. Her research interests are energy conversion materials and devices, and *in situ* temperature measurement instruments for aeroengine turbine blades.

Dr. Niu was a recipient of the First Level Prize of 2020 Science and Technology Progress Award for Natural Science of Sichuan Province.

Shan Gao was born in Yichun, Heilongjiang, China, in 1986. He received the B.S. degree in electronic information engineering and the M.S. degree in communication and information systems from Harbin Engineering University, Harbin, China, in 2009 and 2012, respectively, and the Ph.D. degree from the School of Electrical Engineering and Automation, Harbin Institute of Technology, Harbin, in 2017.

He is currently an Assistant Professor with the College of Information and Communication Engineering, Harbin Engineering University. His current research interests include optical detection technology, artificial intelligence, and engine measurement technology.

Jing Jiang received the B.S. degree in optical information science and technology and the Ph.D. degree in optical engineering from the University of Electronic Science and Technology of China, Chengdu, China, in 2003 to 2013, respectively.

From 2013 to 2018, she was a Lecturer with the University of Electronic Science and Technology of China, where she was an Associate Researcher, from 2018 to 2020, and has been a Researcher since 2020. She has authored more than 30 peer-reviewed journal articles in high-impact journals. Her research interests include *in situ* multiparameters measurement instruments for semiconductor epitaxial growth, *in situ* temperature measurement instruments for aeroengine turbine blades, and energy conversion materials and devices.

Dr. Jiang was awarded the Fifth Session Young Talents Lifting Project of China Association for Science and Technology, the First Level Prize of 2019 Technological Invention in Science and Technology Award of Chinese Institute of Electronics, and the First Level Prize of 2020 Science and Technology Progress Award for Natural Science of Sichuan Province.

Zezhan Zhang received the B.E. degree in electrical engineering and automation from Southwest Minzu University, Chengdu, China, in 2016, and the M.S. degree in materials science and engineering from the University of Electronic Science and Technology of China, Chengdu, in 2019, where he is currently pursuing the Ph.D. degree in electronic science and technology.

His research interest is radiation temperature measurement technology for dynamic targets in extreme environments, including 2-D temperature field measurement of aeroengine turbine blades, radiation temperature measurement technology for turbine disks, and research on high-temperature emissivity characteristics of superalloy materials.

Peifeng Yu received the B.E. degree in mechanical engineering from Southwest Petroleum University, Chengdu, China, in 2015, and the M.S. degree in mechanical and transportation engineering from the China University of Petroleum, Beijing, China, in 2018. He is currently pursuing the Ph.D. degree in electronic science and technology with the University of Electronic Science and Technology of China, Chengdu.

His research interests include the dynamic simulation and analysis of marine catenary risers, and noncontact measurement of strain parameters in extreme environments.

Hairong Dong (Senior Member, IEEE) received the B.S. and M.S. degrees in automatic control and basic mathematics from Zhengzhou University, Zhengzhou, China, in 1996 and 1999, respectively, and the Ph.D. degree in general and fundamental mechanics from Peking University, Beijing, China, in 2002.

She was a Visiting Scholar with the University of Southampton, Southampton, U.K., in 2006, The University of Hong Kong, Hong Kong, in 2008, the City University of Hong Kong, Hong Kong, in 2009, The Hong Kong Polytechnic University, Hong Kong, in 2010, and the KTH Royal Institute of Technology, Stockholm, Sweden, in 2011. In 2007, she served as a Project Level-3 Expert with the Department of Transportation for the Beijing Organizing Committee for the Olympic Games, Beijing. She is currently a Professor with the State Key Laboratory of Rail Traffic Control and Safety, Beijing Jiaotong University, Beijing. Her current research interests include stability and robustness of complex systems, control theory, intelligent transportation systems, automatic train operation, and parallel control and management for high-speed railway systems.

Dr. Dong is a member of IEEE Intelligent Transportation Systems Society, Society of Intelligent Aerospace Systems, Chinese Society of Aeronautics and Astronautics, and Chinese Automation Congress.